This article has been accepted for publication in MNRAS © 2018 The Authors. Published by Oxford University Press on behalf of the Royal Astronomical Society. All rights reserved.

Monthly Notices of the ROYAL ASTRONOMICAL SOCIETY

MNRAS **480,** 3907–3915 (2018)
Advance Access publication 2018 July 24

doi:10.1093/mnras/sty1968

Probing the origin of extragalactic magnetic fields with Fast Radio Bursts

F. Vazza,[1,2,3★] M. Brüggen,[2] P. M. Hinz,[2,4] D. Wittor,[1,2,5] N. Locatelli[1,4] and C. Gheller[6]

[1]*Dipartimento di Fisica e Astronomia, Universitá di Bologna, Via Gobetti 93/2, I-40121, Bologna, Italy*
[2]*Hamburger Sternwarte, University of Hamburg, Gojenbergsweg 112, D-21029 Hamburg, Germany*
[3]*INAF - Istituto di Radioastronomia, Via Gobetti 101, I-40129 Bologna, Italy*
[4]*Universitäts-Sternwarte München, Scheinerstr. 1, D-81679 München, Germany*
[5]*INAF - Osservatorio di Astrofisica e Scienza dello Spazio di Bologna, Via Gobetti 93, I-40129 Bologna, Italy*
[6]*CSCS-ETHZ, Via Trevano 131, 6900 Lugano, Switzerland*

Accepted 2018 July 19. Received 2018 July 17; in original form 2018 May 25

ABSTRACT

The joint analysis of the Dispersion and Faraday Rotation Measure (RM) from distant, polarized Fast Radio Bursts (FRBs) may be used to put constraints on the origin and distribution of extragalactic magnetic fields on cosmological scales. While the combination of Dispersion and Faraday RM can in principle give the average magnetic fields along the line-of-sight, in practice this method must be used with care because it strongly depends on the assumed magnetization model on large cosmological scales. Our simulations show that the observation of RMs with $\geq 1 - 10$ rad m^{-2} in $\sim 10^2$–10^3 FRBs will likely be able to discriminate between extreme scenarios for the origin of cosmic magnetic fields, independent of the exact distribution of sources with redshift. This represents a strong case for incoming (e.g. ALERT, CHIME) and future (e.g. with the Square Kilometer Array) radio polarization surveys of the sky.

Key words: methods: numerical – galaxies: clusters: general – intergalactic medium – large-scale structure of Universe.

1 INTRODUCTION

Fast radio bursts (FRBs) are powerful (∼Jy), dispersed, and intermittent bursts of radio waves, whose origin has yet to be understood. They are often found at high Galactic latitudes and characterized by very large values of dispersion measure (DM), which suggests that they are of extragalactic origin (Lorimer et al. 2007; Thornton et al. 2013; Petroff et al. 2016). According to recent estimates, an FRB may occur at each second within the observable Universe (Fialkov & Loeb 2017). As they traverse the intergalactic medium, the dispersion of radio waves from extragalactic FRB can help detect the missing baryonic matter in the Universe (McQuinn 2014).

If the sources of FRB are at cosmological distances ($z_{\rm FRB} \sim$ 0.2–2), their estimated isotropic release of energy is in the range of $\sim 10^{40}$–10^{42} erg s^{-1}. However, there is no consensus yet concerning their emission mechanisms (Lyubarsky 2014; Kumar, Lu & Bhattacharya 2017; Ghisellini & Locatelli 2017). FRB can be used for cosmological parameter studies (Walters et al. 2017), and the simultaneous detection of their Faraday Rotation Measure (RM) and their DM will make it possible to infer the average magnetic field along the line-of-sight (LOS, Dolag et al. 2015; Petroff et al. 2017).

Unlike the analysis of RM from polarized radio galaxies, the brightness of FRB allows us to probe lower values of RM and to measure the rotation of their polarization angle with higher accuracy. Only a few dozen FRB have been detected so far, and only for a handful of them it has been possible to measure the corresponding RM (Petroff et al. 2016). However, the situation is expected to improve dramatically with ongoing (Petroff et al. 2015; Keane et al. 2017) and future (Trott, Tingay & Wayth 2013, see also ALERT survey with Aperitif) radio surveys, specifically designed to detect FRB, with an expected detection rate of a few FRB per day.

The possible role of FRB to explore extragalactic magnetic fields is particularly important as the distribution of magnetic fields beyond the scale of galaxies and clusters of galaxies is still largely unknown. In cosmic voids, magnetic fields are constrained to be within upper limits of order ∼nG, derived from the Cosmic Microwave Background (Planck Collaboration et al. 2016), and possibly above the lower limits inferred by the absence of Inverse Compton Cascade from distant blazars (Dai et al. 2002; Caprini & Gabici 2015), of order $\sim 10^{-7}$ nG. In filaments of the cosmic web, only limits at the level of a few ∼nG have been inferred from radio observations (Planck Collaboration et al. 2016; Pshirkov, Tinyakov & Urban 2016; Vernstrom et al. 2017). Any detection of magnetic fields beyond galaxies and galaxy clusters will help to explore the origin of cosmic magnetism (Vazza et al. 2015, 2017) by distinguishing between primordial processes in the early Universe (Kahniashvili,

★ E-mail: franco.vazza2@unibo.it

© 2018 The Author(s)
Published by Oxford University Press on behalf of the Royal Astronomical Society

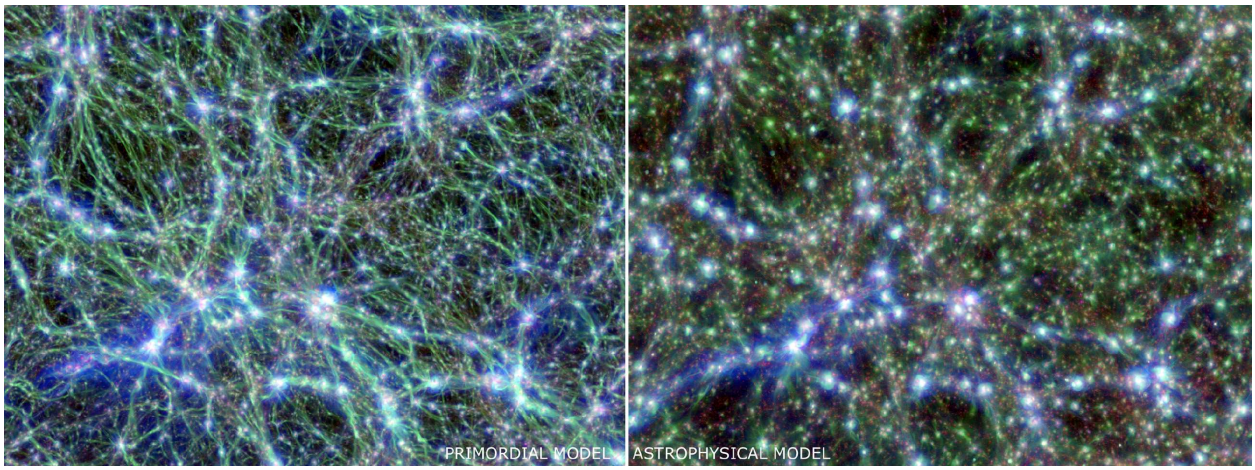

Figure 1. Three-dimensional renderings of the projected distribution of dark matter (red), gas temperature (blue), and magnetic field strength (green) at $z = 0.02$ for the primordial and astrophysical model investigated in this paper. Each panel is 60 Mpc × 40 Mpc across, and has a depth of 200 Mpc along the line of sight.

Tevzadze & Ratra 2011; Widrow et al. 2012; Subramanian 2016), or more local astrophysical processes related to galaxy formation (Donnert et al. 2009; Xu et al. 2009).

Due to the very weak radio signal expected outside of haloes, other methods have been proposed to probe extragalactic magnetic fields, such as by studying Ultra High Energy Cosmic Rays (Dolag et al. 2005; Hackstein et al. 2017; Bray & Scaife 2018). Common with this approach is that neither for Ultra High Energy Cosmic Rays nor for FRB the sources are known. In this study, we rely on some very simple assumptions about the distances to the sources and we use new cosmological simulations of extragalactic magnetic fields to study the opportunities and intrinsic limitations that a future large number of detected FRB in Faraday Rotation will offer to the study of the distribution and origin of extragalactic magnetic fields. This paper is structured as follows: after describing our simulations and numerical tools in Section 2, we present our results in Section 3. We provide physical and numerical caveats in Section 4 before we summarize and conclude our work in Section 5.

2 METHODS

2.1 Numerical simulations

We simulated the evolution of dark and baryonic matter as well as cosmic magnetic fields using the ENZO code (Bryan et al. 2014). The simulation covered a 200^3 Mpc^3 (comoving) volume using 2400^3 cells and dark matter particles, achieving the constant comoving resolution of 83.3 kpc cell^{-1} and the constant mass resolution of $m_{\rm DM} = 6.19 \cdot 10^7$ M$_\odot$ per dark matter particle.

In order to best bracket uncertainties, we employ here two different models of gas physics and magnetic fields, similar to Vazza et al. (2017). The first is a non-radiative run with a primordial scenario for magnetic fields, in which we initialized a uniform magnetic field of 10^{-9} G (comoving) already at the start of the simulation ($z_{\rm in} = 38$) and let it evolve under the effect of gravity and magnetohydrodynamical forces. In the second model, the astrophysical scenario, we use radiative simulations including a simple prescription for feedback from active galactic nuclei (AGN). Now the initial seed field is 100 times smaller (10^{-11} G comoving) and the gas can cool via equilibrium cooling assuming a primordial composition. When cooling pushes the gas density above $n_{\rm th} = 10^{-2}$ part cm^{-3} (typical of cool core galaxy clusters), bipolar thermal jets with a fixed budget of $E_{\rm AGN} = 10^{58}$ erg of thermal energy (and $E_{\rm B} = 1$ per cent $E_{\rm AGN}$ of magnetic energy) are launched to mimic the large-scale effects of AGN self-regulation of cluster atmospheres. Even though the second scenario also includes a weak primordial seed field, for simplicity we refer to it as 'astrophysical' as the resulting present-day magnetic fields in large-scale structures are dominated by the injection and amplification of magnetic fields seeded at low redshifts by AGN.

In previous work, we have shown how this implementation is fairly effective in reproducing the $M-T$ scaling relation on the high-mass end and on the low-mass end of observed clusters, large-scale profile of density and temperature in clusters (Vazza, Brüggen & Gheller 2013; Vazza et al. 2016), as well as the observed distribution of radio relic sources (Vazza et al. 2015). For a discussion on the comparison of this approach to more sophisticated models based on supermassive black hole particles, we refer the reader to Vazza et al. (2017).

Fig. 1 shows the large-scale distribution of dark matter, gas temperature, and magnetic fields in the two scenarios. The differences between the thermal and magnetic properties of the haloes are small across runs, while the differences (especially in magnetic fields) become increasingly large moving into the more rarefied environment of filaments and voids. We find that in the primordial case under-dense regions show a $\sim 10-10^2$ higher magnetic field values than the run with feedback.

In all runs, we assumed a lambda cold dark matter cosmological model, with density parameters $\Omega_{\rm BM} = 0.0478$, $\Omega_{\rm DM} = 0.2602$, $\Omega_\Lambda = 0.692$, and a Hubble constant $H_0 = 67.8$ km sec^{-1}Mpc^{-1} (Planck Collaboration et al. 2016).

In Section 4.4, we will also discuss further simulations that include other models for seed fields.

2.2 Simulated Rotation and DMs

We compared the RM and DM of both resimulations by extracting 1000 one-dimensional beams of cells along the z-axis of the simulation at random x, y-positions (identical for the two runs). Since the redshift distribution of observed FRB is still unknown (Oppermann, Connor & Pen 2016; Fialkov & Loeb 2017; Walker, Ma & Breton 2018), we tested three different procedures to locate FRB sources in

the simulation. In the first, simple model, we assumed all FRB are located at redshift $z = 2$ ($d_L = 15.8$ Gpc). In the second model, we randomly extracted the redshift of sources from a distribution that follows the observed cosmic star formation rate (SFR) as a function of redshift, which is well approximated by $P(SFR) \propto z^3$ for $z \leq 2$ (Madau & Dickinson 2014), assuming a maximum distance of $z = 2$. In the third model, we have randomly drawn sources assuming they are uniformly distributed in comoving radial distance. In order to generate LOS from $z = 0.02$ to $z = 2.0$, we concatenated 26 beams of 2400 cells each taken from outputs at different redshift, for a total comoving distance of ≈5.2 Gpc. Given that our computational box has a fixed comoving volume, our corresponding sampling Δz is discontinuous, and goes from $\Delta z \approx 0.045$ at $z = 0.02$ to $\Delta z \approx 0.2$ towards $z = 2$. In order to avoid artefacts caused by the periodic repetition of structures along each LOS from $z = 2$ to $z = 0.02$, we concatenated 26 different LOS crossing the 200^3 Mpc^3 box from random positions at increasing redshift. Of course, the discrete sampling in redshift causes artefacts (especially in the magnetic field distribution) at the boundaries of each box. However, considering that the fraction of cells close to boundaries is $8 \cdot 10^{-4}$ of the total number of cells for each LOS, the artefacts introduced at the edges have a negligible effect on the resulting DM and RM.

Each of the 1000 LOS consists of 62 400 cells with a continuously interpolated distribution of redshift, and physical values of lengths, density, and magnetic fields based on this redshift distribution.

The DM for each LOS is defined as:

$$DM\ [\mathrm{kpc/cm^3}] = \int_0^{\mathrm{d_{FRB}}} \frac{\mathrm{n_e(z)}}{(1+\mathrm{z})\ \mathrm{cm^3}} \frac{\mathrm{dl}}{\mathrm{kpc}}, \quad (1)$$

where d_{FRB} is the assumed comoving distance of each FRB, z is the redshift of each cell, and n_e is the physical electron density of cells, assuming a primordial chemical composition ($\mu = 0.59$) of gas matter everywhere in the volume. The values of DM along a simulated LOS are given in the first panel of Fig. 3: the differences between the same LOS in our two models are extremely small as the gas density distribution on such scales is hardly affected by cooling or feedback.

We should point out that the standard analysis of DM (Ioka 2003) often assumes a uniform and completely ionized distribution of baryons, which allows to simplify equation (1) to $z_{FRB} = \mathrm{DM}/1200\ \mathrm{pc\,cm^{-3}}$ (which is valid up to $z = 2$ with a very small ∼2 per cent scatter). However, from the distribution of DM from our reference $z = 2$ model in Fig. 2 we can clearly see that even when all FRB are located at the same distance, the observed scatter in DM is large (∼30 per cent) as most of the cosmic volume is underdense, and the number of overdense structures that are crossed by each LOS introduces a substantial deviation on the final DM of each source.

The RM for each LOS is defined as:

$$RM\ [\mathrm{rad\,m^{-2}}] = 812 \int_0^{\mathrm{d_{FRB}}} \frac{\mathrm{B_{||}}}{\mu\mathrm{G}} \cdot \frac{\mathrm{n_e}}{(1+\mathrm{z})\ \mathrm{cm^3}} \frac{\mathrm{dl}}{\mathrm{kpc}}, \quad (2)$$

where || denotes the component of the magnetic field parallel to the LOS. The observed DM and RM of a single extragalactic FRB have contributions from the local environment of the source, its host galaxy, the intergalactic medium, and finally the Milky Way (Akahori, Gaensler & Ryu 2014). In what follows, we only consider the contribution from the intergalactic medium.

The panels in Fig. 3 shows the integrated DM and |RM| from $z = 1$ to $z = 0.02$ for the same LOS. While the DM is consistent at all redshifts within a few per cent in the two cases, the |RM| clearly differs, with the marked tendency of the primordial model to show a higher |RM| at all redshift. Only close to the sites where magnetic fields are injected by AGN, localized in the highest density peaks of the simulated volume, the |RM| in the two models become similar. This trend is consistently found in most LOS: the RM difference between the same set of LOS is typically larger than the cosmic variance within models. Fig. 4 shows the sample variance for 100 LOS integrated from $z = 0$ to $z = 1$, where a clear segregation in RM (unlike in DM) is measured in the two scenarios. This behaviour indicates already that any inversion of the |RM|/DM relation to obtain the average magnetic field along the LOS will give different results, depending on the physical model for the origin of extragalactic magnetic fields.

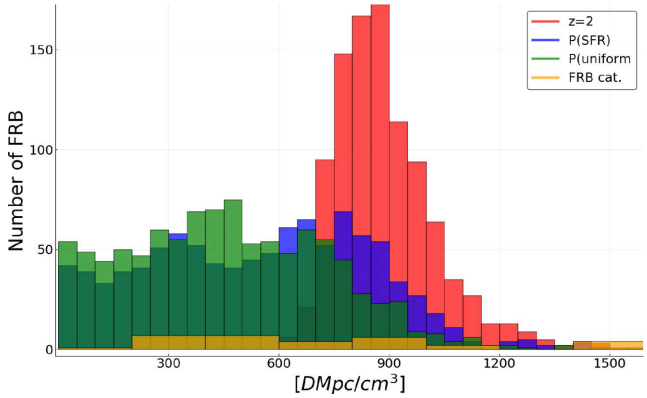

Figure 2. Distribution of DM in observed FRB (Petroff et al. 2016) (after removing from the putative contribution from the Milky Way) and simulated in this work, by assuming three different models for the location of sources (see Section 2.1).

Fig. 2 gives the distribution of the DM for our three source models for FRBs, compared with the presently known distribution of FRBs based on the *FRBcat Catalog*(http://frbcat.org), where we considered the DM of each FRB after removing the putative $\mathrm{DM_{MW}}$ from the Milky Way (Petroff et al. 2016). The latter contribution is derived using the electron density model by Cordes & Lazio (2002), while the intrinsic contribution from the hosts of FRB is unknown (see e.g. Walker et al. 2018, for a recent discussion), and is therefore neglected, consistently with our simulated data. While none of our models are successful in reproducing the observed distribution of DM in real FRB, which shows no clear dependence on DM, the model based on the cosmic SFR yields a slightly larger fraction of DM ≥ 800 − 1000, similar to observed statistics (Petroff et al. 2016).

2.2.1 *Higher resolution data*

While these simulations are among the largest and, certainly in the underdense regions, most resolved cosmological simulations of extragalactic magnetic fields, our computational grid is too coarse to properly model the growth of magnetic fields in galaxy clusters, which is governed by a small-scale dynamo (Beresnyak & Miniati 2016). The simulation of a small-scale dynamo requires a fairly large effective Reynolds number, which is still difficult to achieve, certainly in simulations of cosmological scales (Vazza et al. 2018). In order to include the role of magnetic field amplification within massive haloes for a subset of our fiducial runs, we replaced the magnetic field values from cells located in overdensities typical for clusters by those from higher resolution runs (∼4 kpc cell^{-1})

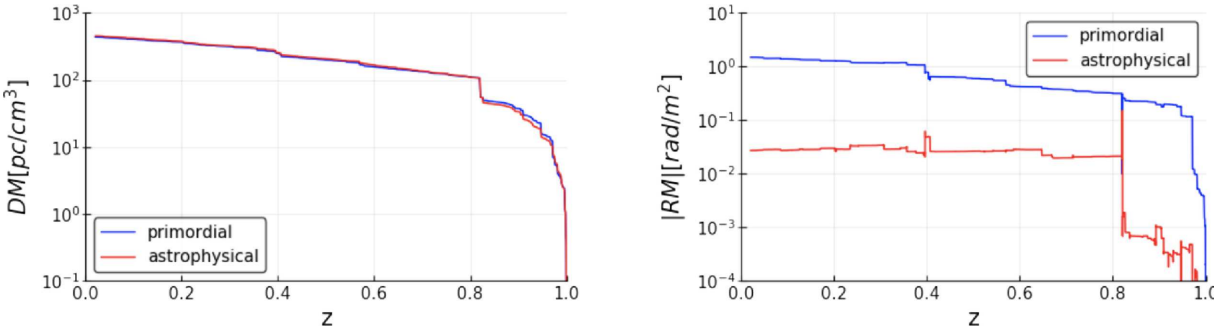

Figure 3. DM and RM along one representative LOS in the two models considered in this work, for a sample source located at $z = 1$.

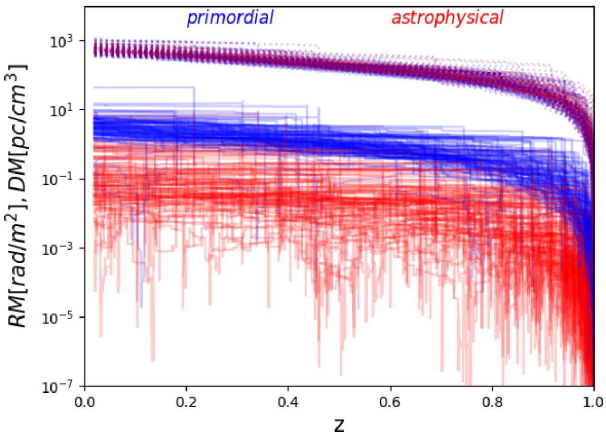

Figure 4. Trend of DM and RM for 100 simulated LOS in the two models considered in this work, for sources located at $z = 1$. The top dotted lines show the trend of DM, while the lower solid lines give the trend of RM.

(Vazza et al. 2018). This experiment is only performed for the non-radiative simulation with a primordial magnetic field.

In particular, we identified all cells with a gas density larger than the typical gas density at the virial radius of self-gravitating haloes ($\rho \geq 50\rho_{c,b}$ where $\rho_{c,b}$ is the cosmic baryon critical density at a given redshift) and randomly replaced both their density and magnetic fields by randomly drawing from LOS taken from the adaptive mesh refinement (AMR) simulation. This nested procedure approximates a full AMR simulation with ∼4−5 levels of refinement on top of our baseline 83.3 kpc resolution.

3 RESULTS

We start by analysing the distribution of observable DM and |RM|, as shown in Fig. 5. In Table 1, we give the best-fitting parameters for a simple $\log_{10}(|\mathrm{RM}|) = \alpha + \beta \cdot \log_{10}(\mathrm{DM})$ relation, for all models and source distributions considered here.

The two models of magnetic fields fill the (|RM|,DM) plane in different ways. The primordial model tends to produce larger RM values for DM ≤ 600 pc cm^{-3} while the astrophysical model produces a larger scatter of values at any DM. Remarkably, in the primordial scenario the different distribution of sources yields the same best-fitting relation, of the kind

$$\frac{|\mathrm{RM}|}{\mathrm{rad\,m^{-2}}} \approx 10^{-4} \left(\frac{\mathrm{DM}}{\mathrm{pc\,cm^3}}\right)^{1.3\div1.5}, \tag{3}$$

with exact parameters given in Table 1. A very similar relation, albeit with a larger scatter, also holds for the astrophysical models, with the exception of the $z = 2$ source model, which shows a steeper slope ($\beta \sim 4.6$). This can be understood because $z = 2$ is close to the peak of simulated AGN activity. Hence LOS is more likely to cross magnetized bubbles released by AGN which consequently yield larger RM.

The situation is reversed if we only look at $|\mathrm{RM}| \geq 0.1$ rad m^{-2}, which is the only part of the RM space that observations in the foreseeable future might be able to probe. As expected, the highest RMs are found in the astrophysical model. This is a result of higher densities that are found in radiative simulations as well as a result of stronger magnetic fields close to higher density regions that experience AGN feedback. Also we find a much larger scatter of RMs in the astrophysical model.

If we go to low RMs ($|\mathrm{RM}| \geq 1 - 10$ rad m^{-2}) which might enter the parameter space probed by SKA-MID, the distribution of FRB in the (|RM|,DM) plane will have the potential to discriminate among such extreme scenarios: while in the primordial case we expect a small scatter around $\sim 1 - 2$ rad m^{-2} for sources with DM ≥ 1000 pc cm^{-3}, we expect possible variations up to ∼2 orders of magnitude in RM ($|\mathrm{RM}| \sim 0.2 - 20$ rad m^{-2}), for the same range of DM, irrespective of the exact distribution of sources. In particular, while in the primordial scenarios we expect that |RM| values from the cosmic web should be clustered around $DM \approx 900$ pc cm^{-3} and $|\mathrm{RM}| \approx 1$ rad m^{-2}, factor ∼5−10 times larger RMs may be expected in the astrophysical scenarios, nearly independent of their DMs.

Already with a few tens of sources in this (|RM|, DM) range, it will be possible to falsify models of extragalactic fields, even without a detailed knowledge of the intrinsic redshift of the sources, as shown in Fig. 6.

Our results point towards the possibility of studying the origin of cosmic magnetism using FRB through the observed scatter of RMs. However, they also imply that FRB is not a trustworthy probe of the magnetization of the intergalactic medium along the LOS. Even without taking into account the potential role of the unknown contribution of DM and RM by their host galaxies, the (|RM|,DM) relation given by our simulations, irrespective of the exact distribution of sources, is affected by a large scatter. We combined the mock RM and DM values of all simulated FRB in our sample, and estimate the magnetic field along each LOS as:

$$B_{\mathrm{RM/DM}} = \frac{1000\ \mathrm{pc\,cm^{-3}}}{812\ \mathrm{rad\,m^{-2}}} \cdot \frac{|\mathrm{RM}|}{\mathrm{DM}}. \tag{4}$$

This can be compared to the real rms value of magnetic fields along each LOS ($\sigma_{\mathrm{B,\,true}}$). The results are shown in Figs 7 and 8. In both scenarios and fairly independently on the redshift distribution of sources, the *intrinsic* scatter in $B_{\mathrm{RM/DM}}/\sigma_{\mathrm{B,\,true}}$ is large, ∼1 order of magnitude in the primordial case and ∼2 in the astrophysical

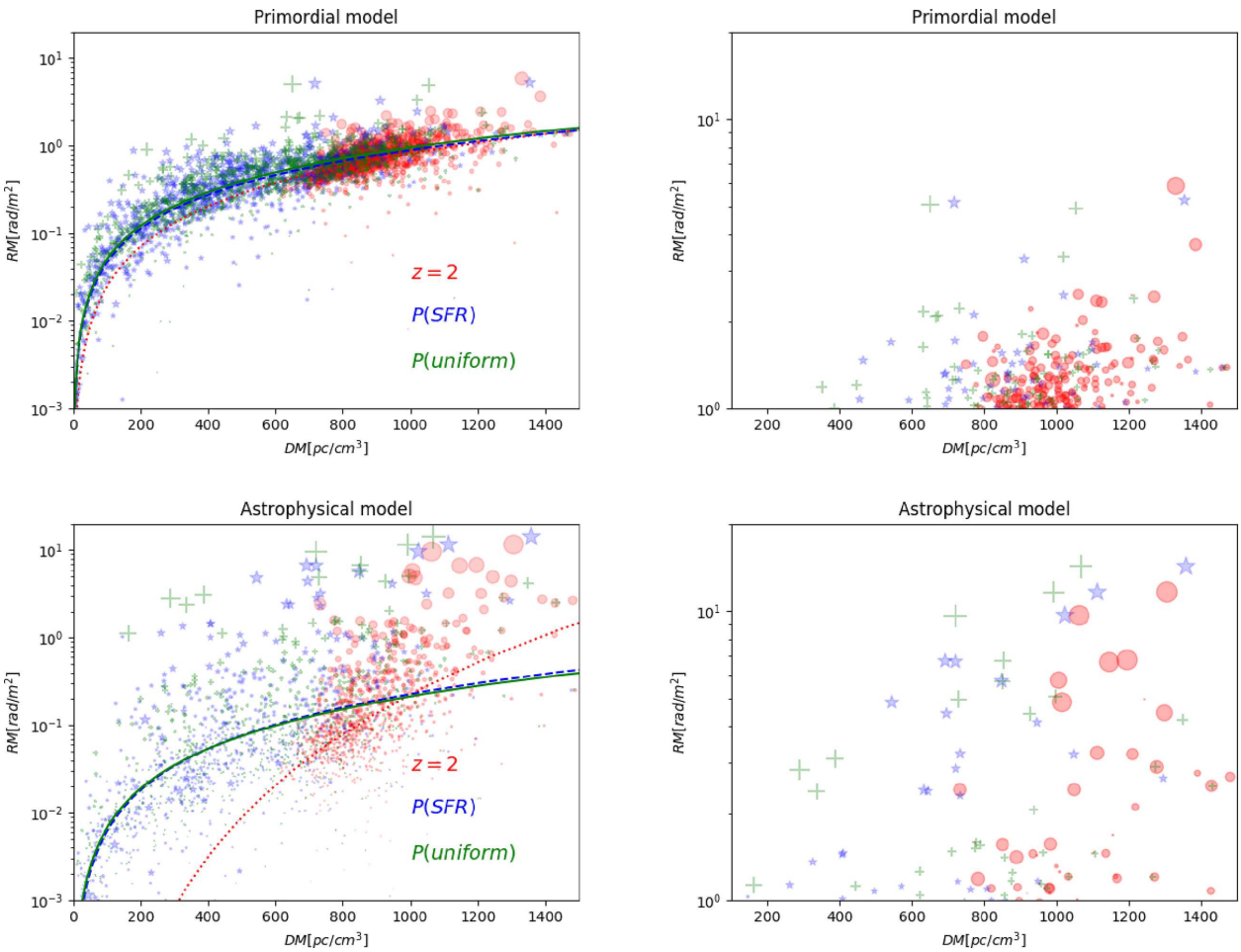

Figure 5. RM versus DM for 1000 LOS in the primordial scenario (top panels) and in the astrophysical scenario (bottom panels) scenario. The different colours and symbols denote different models for the distribution of FRB. The right plots give the close-up view of the high |RM| region of the plots, which might be observable with SKA-MID. The size of markers linearly scales with the average strength of the magnetic field along each LOS.

Table 1. Best-fitting parameters for the $\log_{10}|\mathrm{RM}| = \alpha + \beta \cdot \log_{10}\mathrm{DM}$ relations (with 1σ deviation) in the various models and runs explored in this work.

B-field model	source model	α	β
Primordial	$z = 2$	-4.65 ± 0.46	1.52 ± 0.15
Primordial	P(SFR)	-3.90 ± 0.08	1.28 ± 0.03
Primordial	P(uniform)	-3.90 ± 0.09	1.28 ± 0.03
Astrophysical	$z = 2$	-14.62 ± 1.14	4.66 ± 0.38
Astrophysical	P(SFR)	-5.35 ± 0.17	1.57 ± 0.07
Astrophysical	P(uniform)	-5.22 ± 0.19	1.50 ± 0.07

scenario. Moreover, in the primordial case the peak of the observed distribution of $\sigma_{\mathrm{B,\,true}}$ is systematically biased high by a factor $\sim$4−5 with respect to the real value measured along each LOS. This bias is nearly absent (≤ 2) in the astrophysical scenario, yet the very large scatter in the reconstructed values makes it too uncertain to rely on equation (4).

We note that Akahori, Ryu & Gaensler (2016) have suggested to recalibrate equation (4) in order to recover the average magnetic field along LOS probed by FRB, by introducing a weighting factor, $\langle 1 + z \rangle\ f_{\mathrm{DM}}$, where f_{DM} is the fraction of DM produced by the gas phase in the 10^5 K $\leq$ T $\leq 10^7$ K range, which was mostly responsible for the observed (|RM|, DM) values found in their simulated LOS. In particular, they discussed one specific model where extragalactic magnetic fields are predicted based on the phenomenological use of magnetic field amplification efficiency factors, derived from turbulence-in-a-box simulations (Ryu et al. 2008), and are not the result of full MHD simulations.

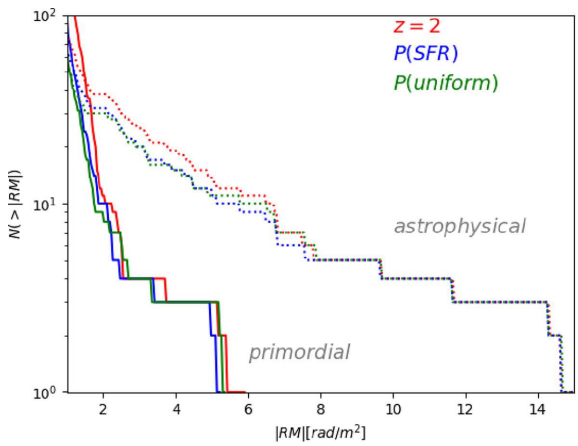

Figure 6. Distribution of |RM| for ≥ 1 rad m^{-2} data in our sample.

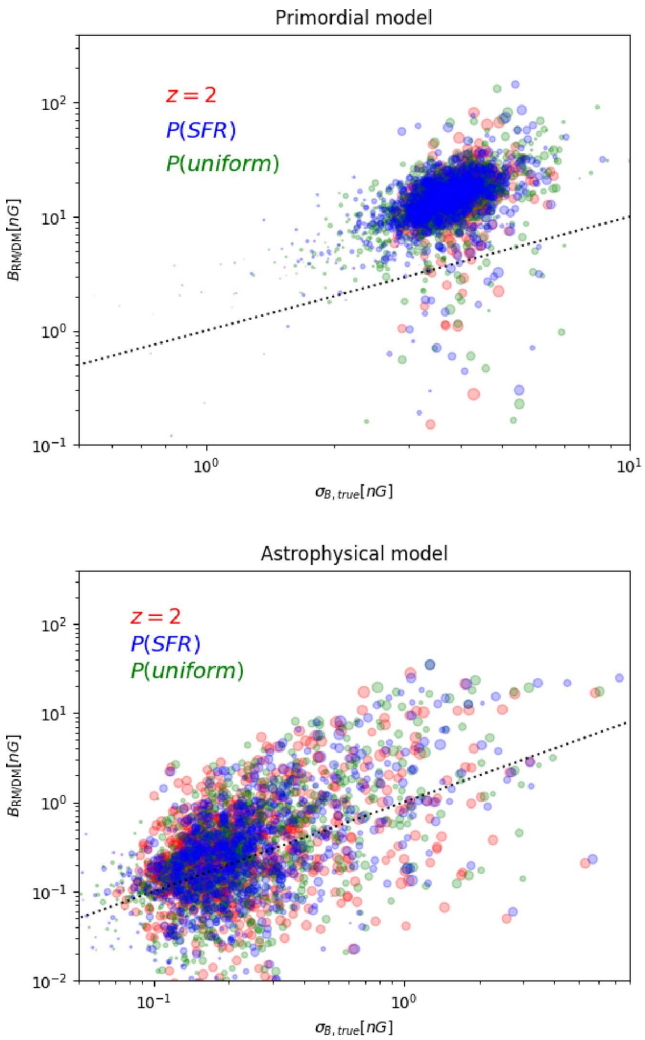

Figure 7. Relation between the rms magnetic field along the LOS and the magnetic field, which is inferred from the combination of RM and DM, comparing primordial (top) and astrophysical (bottom) scenarios for the different investigated source models. The size of dots correlates with the DM along each LOS.

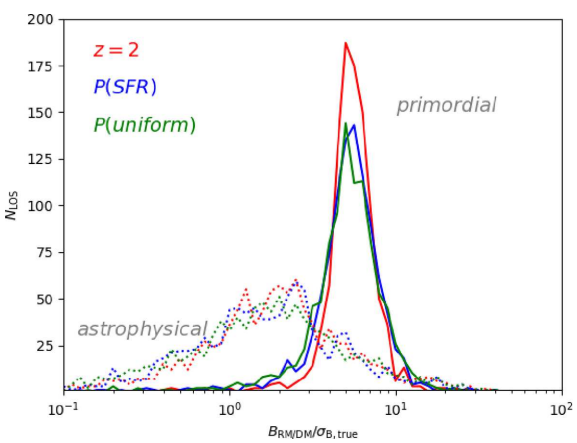

Figure 8. Distribution of the ratio between the average magnetic field inferred from the B(RM/DM) relation and the true one for our simulated LOS.

The differences in our models can account for the reported differences in the use of the (|RM|, DM) relation to measure cosmic magnetism. In the Akahori et al. (2016) model the magnetization of filaments (assumed in post-processing as a regular function of cosmic environment) dominates the signal along the LOS. Hence, by assessing the typical relation between the cosmic density of filaments and their magnetization, it is possible to calibrate the (|RM|, DM) relation to infer magnetic fields with good precision. Conversely, our results show that there is no single correction factor to calibrate the (|RM|, DM) relation. Firstly, even in the primordial scenario we observe that the local dynamics of filaments can introduce a significant scatter in their final magnetization, even within the same range of overdensities. Secondly, in the assumed primordial scenario, the contribution to the RM along LOS up to z = 2 is not entirely due to gas in the $10^5 - 10^7$ K range as in Akahori et al. (2016). Hence, there is no single gas phase that can be used to reliably calibrate the (|RM|, DM) relation. Finally, AGN activity can introduce an even larger source of scatter in the observable (|RM|, DM) relation because, for a given cosmic overdensity, the local magnetic field can vary, based on the preceding AGN activity.

4 PHYSICAL AND NUMERICAL CAVEATS

4.1 Astrophysical uncertainties

An unavoidable limitation of our analysis is that the contributions to DM and RM by the FRB hosts remain unknown, and they are expected to strongly depend on the morphology of the host galaxy as well as on the exact location of the FRB within it (Walker et al. 2018). While the Milky Way halo is expected to contribute to $DM_{MW} \sim 40 \pm 15$ pc cm^{-3} (Dolag et al. 2015), hosts of FRB are expected to contribute more to the DM (Xu & Han 2015). For example, a host DM contribution of ∼250 pc cm^{-3} has been suggested for the repeating FRB 12110, which is localized in the star-forming region of a $z = 0.19$ dwarf galaxy (Chatterjee et al. 2017). For sources located within $z \leq 2$, Walker et al. (2018) suggested that a DM in the range of $DM_{host} \sim 50$–500 pc cm^{-3} might be expected for reasonable variations of possible progenitors and location within host galaxies.

Another unavoidable source of uncertainty in radio observations results from the Galactic foreground. Studying the redshift dependence of RM in a large sample of quasars, Han (2017) recently suggested that up to $\sim 10^4$–10^5 measurements of RMs may be necessary to tell apart Galactic from extragalactic contributions to the dispersion of RMs in distant objects. FRBs may ease this requirement because they may be distributed more evenly at low redshift ($z \leq 1$) than quasars. Moreover, it is expected that our knowledge of the three-dimensional structure of the Galactic magnetic field will improve at the same pace as RM statistics, thus improving templates of the Galactic foreground screen. For example, the combination of several set of observables (such as extragalactic RMs, PLANCK polarization data, galactic synchrotron emission, and observed distribution of ultra-high energy cosmic rays) through Bayesian inference already allows considerable improvements in the reconstruction of Galactic magnetic fields across a wide range of scales (Boulanger et al. 2018, for a recent review).

4.2 Numerical uncertainties

Because of the finite numerical resolution, any simulation will be agnostic about fluctuations below a given cell size. In the case of

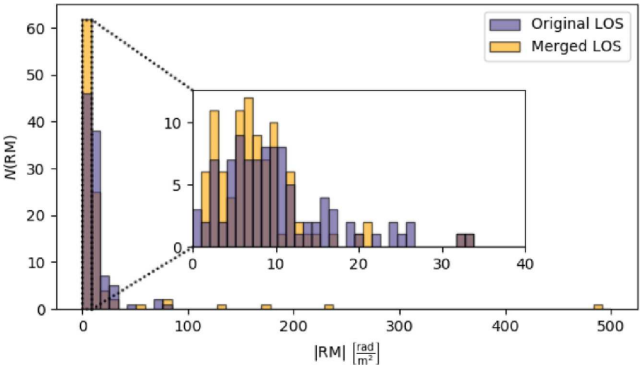

Figure 9. Distribution of the RM for 100 simulated LOS, where limited to high-density regions we replaced the magnetic field values of the simulation used in the main paper (with a fixed spatial resolution of 83 kpc comoving) with highest resolution data from an AMR run simulation of a 10^{15} $M_\odot$ galaxy cluster (with the peak resolution of 3.9 kpc comoving). The RM obtained using this combined data set ('merged LOS') are contrasted with the original RM in the simulation.

MHD simulations, an additional problem is that small-scale magnetic field fluctuations are seeded by the *inverse* cascading of magnetic energy from small to large scales, if the flow is in the small-scale dynamo regime. This is observed in the case of galaxy clusters, simulated at sufficiently high (≤ 10 kpc) spatial resolution (Vazza et al. 2018). The constant resolution of 83.3 kpc cell^{-1} (comoving) is sufficient to represent voids, sheets, and filaments, where previous studies found no evidence of small-scale dynamo amplification driven by structure formation even at higher resolution (Vazza et al. 2014).

As discussed in Section 2.2.1, we have investigated this issue in more detail by replacing the magnetic field and gas density values in 100 of our simulated LOS in the primordial scenario with much higher resolution data (4 kpc) taken from our recent AMR simulations (Vazza et al. 2018). The resulting distribution of RM is shown in Fig. 9. The volume fraction occupied by cluster-like regions is small in our random distribution of LOS, and beside a few |RM| $\sim$ 250–500 rad m^{-2} values (found in LOS clearly piercing the centre of galaxy clusters) the overall statistics of RM values is unchanged (similar results are found for the DM statistics). This is further confirmed by computing the fractional contribution to DM and |RM| from cells with a gas density higher than the virial one along our LOS. Cells in the cluster-like environment are found to contribute on average only to a $\sim$2.5–5 per cent of the observed DM, and to $\sim$15.6 per cent of the observed |RM|.

The low contamination of galaxy clusters to the overall distribution of DM and RM values for long LOS is consistent with the expected number of galaxy clusters from cosmology. In recent work, Zandanel et al. (2018) estimated the counts of galaxy clusters with masses $\geq 10^{13}$ $M_\odot$ that are expected for deg^2 as function of redshift. Their integrated counts from $z = 1$ to $z = 0$ yields a total of $\approx$493 clusters deg^{-2}. Normalized to $\sim$0.003 deg^2 area covered by our simulated beams, this gives an average of $n_{\rm cl} \approx 1.48$ clusters per beam. Assuming that each cluster crossing takes on average $l_c = 1$ Mpc, we can estimate an overall $DM_{\rm CL} = 10^2 \cdot n_{\rm cl} \cdot l_{\rm cl} \cdot \langle n \rangle$ contribution to the total DM from $z = 1$ sources, while the contribution from the uniform smooth gas from $z = 0$ to $z = 1$ is $DM = 3.3 \cdot 10^3 {\rm Mpc} \cdot \langle {\rm n} \rangle$. Hence, we can estimate an average contribution of $DM_{\rm cl}/DM \sim 4.4$ per cent from clusters, which is in the range of what we measure in our data ($\sim$2.5–5 per cent).

We conclude that, in general, galaxy clusters do not have a significant effect on the distribution of DM and |RM|.

4.3 Finite resolution of radio observations

A further, important limitation to consider in our modelling is that we assume an *infinitely small* beam size, i.e. we consider for each simulated FRB the effect of a one-dimensional beam of DM and RM values, while in reality an observation with a *finite* beam size will see the convolution of a distribution of values along the integration path from the FRB to the observer. This is an unavoidable assumption of any finite volume method, and in this particular case we are assuming that the structure of magnetic fields and density fluctuations below our cell resolution are negligible compared to the resolved scales. This is reasonable, as the typical Jeans scale for density fluctuations in the intergalactic medium is

$$\lambda_J \approx 1.08 \text{ Mpc} \cdot \sqrt{\frac{T/(10^4 \text{ K})}{\Omega_m(1+\delta)(1+z)}}, \tag{5}$$

and the simulated power spectrum of density fluctuations show very little structure below $\leq$200 kpc even at higher resolution (Lukić et al. 2015). Moreover, also the magnetic field power spectrum in the entire cosmic volume shows little structure below $\leq$1 Mpc (Vazza et al. 2017).

4.4 Additional primordial magnetic models

The results shown so far were obtained for two extreme scenarios for the origin of extragalactic magnetic fields. In Vazza et al. (2017), we presented 20 model variations (for a smaller 85 Mpc^3 volume with identical spatial/mass resolution and cosmology) of extragalactic magnetic fields, and here we present additional tests derived from this suite of simulations. In particular, we compared: (a) the identical non-radiative primordial model as in the rest of the paper; (b) a primordial model in which we impose an initially tangled distribution of magnetic fields, using the Zeldovich approach outlined in the Appendix of Vazza et al. (2017). In this approach, we initialize magnetic fields that correlate with initial density perturbations by generating magnetic field vectors perpendicular to the three-dimensional gas velocity field of the Zeldovich approximation (this way ensuring the $\nabla \cdot \vec{B} \equiv 0$ by construction). The resulting initial magnetic fields have the same power spectrum of the initial velocity fluctuations and is normalized such that $\sqrt{|<B^2>|} = B_0 = 1$ nG. (c) A primordial model starting from the much lower seed field value of $B_0 = 10^{-16}$ G (comoving) but featuring a sub-grid model for a small-scale dynamo (see Appendix of Vazza et al. 2017). In this model, we convert a small fraction η_B ($\leq 5-10$ per cent) of the kinetic energy of the gas solenoidal velocity into magnetic fields. This approach is based on Ryu et al. (2008) and the fitting formulas given by Federrath et al. (2014) that allow us to estimate the effective value of η_B as a function of the flow Mach number. Moreover, we ensure that the newly generated magnetic field is parallel to the direction of the gas vorticity. This model is motivated by the attempt of including a scenario in which small-scale vorticity is generated within cosmic filaments, on scales which presently cannot be directly resolved by cosmological MHD simulations (see. Vazza et al. 2014 for a discussion).

This way we produced analogous sets of 500 LOS for each model.

The resulting (|RM|, DM) relation is shown in Fig. 10. We find that the initial field topology has a small effect on the best-fitting relation for (|RM|, DM), and mainly increases the scatter by a little.

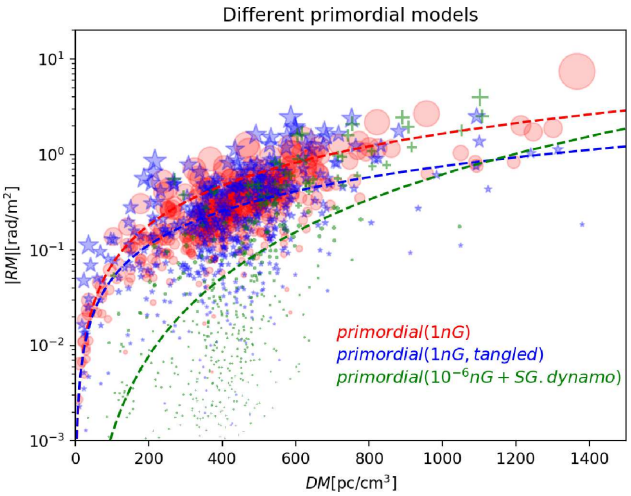

Figure 10. RM versus DM for 500 LOS in three more variations of the primordial scenario (see Section 4.4 for details). The different colours and symbols denote different models for the distribution of FRB. The size of markers linearly scales with the average strength of the magnetic field along each LOS.

The RMs and DMs from FRBs at $z \leq 2$ is relatively independent of the exact topology of the initial magnetic field, while it does depend on the field normalization. Conversely, a scenario in which the primordial seed field is very low and the magnetization is the result of efficient small-scale dynamo amplification even on the scale of filaments (Ryu et al. 2008), results in a steeper (|RM|, DM) relation that falls in between the primordial and the astrophysical model. We conclude that the observed distribution of $|RM|$ is mostly determined by the intermediate overdensity structures of the cosmic web (e.g. filaments), whose magnetization would be systematically impacted by the presence of high primordial fields. By linearly rescaling the level of $|RM|$ observed in our data for lower seed fields, we conclude that virtually no detection of Faraday Rotation from FRBs should be possible for seed fields below $B_0 \leq 0.1$ nG, even if their initial topology is tangled. If the seed fields are much weaker, a systematic detection of Faraday Rotation from the most dispersed (DM $\geq 10^3$ pc cm^{-3}) FRBs should be possible only if some level of small-scale dynamo amplification occurs on $\ll$50 kpc scales. Dynamo amplification on these scales is presently hard to directly simulate with cosmological simulations. No systematic detection of Faraday Rotation from extragalactic FRBs, or a large scatter in the observed (|RM|, DM) relation for large samples would suggest an astrophysical origin for the magnetization of large-scale structures.

5 OBSERVATIONAL PERSPECTIVES AND CONCLUSIONS

We have investigated whether FRBs can be used to study the magnetization of the Universe (Akahori et al. 2016), complementary to the study of radio synchrotron emission from the cosmic web (Vazza et al. 2015; Vernstrom et al. 2017), Ultra-High Energy Cosmic Rays (Sigl, Miniati & Ensslin 2003; Hackstein et al. 2016), or blazar haloes (Dai et al. 2002; Dolag et al. 2009).

Our analysis suggests that the use of the RM–DM relation to infer the magnetization of the intervening matter is not straightforward: the RM–DM relation is typically affected by a large scatter, e.g. at DM $= 10^3$ pc cm^{-3} we typically find a scatter of a factor $\sim$10 for the RM in the primordial scenario, and of $\sim 10^2$ for the astrophysical case. Moreover, due to the non-Gaussian statistics of magnetic field fluctuations in long LOS (Montanino et al. 2017), we find that a simple inversion of the RM–DM relation systematically overestimates the real rms value of magnetic fields along the LOS by a factor $\sim$5−7 in the primordial case, and by a factor of $\sim$2 in the astrophysical scenario. In both cases, the scatter is large ($\sim 10-10^2$).

Consequently, inferring the average magnetization of the intergalactic medium from the combination of observed RM and DM of a few FRB will be prone to large errors, making this procedure quite unreliable. However, for large ($\sim 10^2-10^3$) samples and DM in FRBs there is hope to discriminate at least between a purely primordial and a purely astrophysical scenario, as the dispersion of values in the primordial case is predicted to be $\sim$10 per cent of the dispersion of values in the astrophysical scenario. Remarkably, discriminating between models based on the dispersion of the detected RM values should be possible independent of the distance distribution of sources.

While the DM is only mildly affected by gas physics, the RM depends strongly on the assumed magnetic field model, and has a wider distribution of values in astrophysical scenarios due to the intermittent nature of AGN feedback. We conclude that no systematic detection of Faraday Rotation from extragalactic FRBs, or a large scatter in the observed (|RM|, DM) relation for large samples of FRBs will imply an astrophysical origin for magnetic fields on large scales.

Research on the use of FRB for all kinds of cosmic tomography is still in its infancy, as several experiments are gearing up to detect large numbers of FRB with DM and RM, such as the Canadian Hydrogen Intensity Mapping Experiment (CHIME) which will observe from 400 to 800 MHz, simultaneously using 1024 beams (Ng 2017), or the Aperture Tile in Focus (APERITIF) experiment on the Westerbork telescope, which will observe at 1.4 GHz using $\sim 10^3$ beams (van Leeuwen 2014). When fully operational, also the Square Kilometre Array is expected to produce a breakthrough in the study of FRB: even if extrapolations into its sensitivity range are non-trivial, realistic estimates suggest that up to one FRB per second over the entire sky will be observable using the SKA-MID2 (Fialkov & Loeb 2017). Therefore, when numbers of detected FRB will increase to a few thousands per year, their statistical analysis will make it possible to use FRB as a probe of extragalactic magnetic fields and of the origin of cosmic magnetism.

ACKNOWLEDGEMENTS

The cosmological simulations described in this work were performed using the ENZO code (http://enzo-project.org) that is the product of a collaborative effort of scientists at many universities and national laboratories. We gratefully acknowledge the ENZO development group for providing extremely helpful and well-maintained on-line documentation and tutorials. Most of the analysis done in this work was performed with the JULIA code (https://julialang.org).

F.V. and D.W. acknowledge financial support from the ERC Starting Grant 'MAGCOW', no.714196. We acknowledge the usage of computational resources on the Piz-Daint supercluster at CSCS-ETHZ (Lugano, Switzerland) under project s701 and s805. We thank F. Zandanel, J. L. Han, and T. Akahori for useful scientific feedback, and our anonymous referee for valuable suggestions.

REFERENCES

Akahori T., Gaensler B. M., Ryu D., 2014, ApJ, 790, 123

Akahori T., Ryu D., Gaensler B. M., 2016, ApJ, 824, 105
Beresnyak A., Miniati F., 2016, ApJ, 817, 127
Boulanger F. et al., 2018, preprint (arXiv:1805.02496)
Bray J. D., Scaife A. M. M., 2018 preprint (arXiv:1805.07995)
Bryan G. L. et al., 2014, ApJS, 211, 19
Caprini C., Gabici S., 2015, Phys. Rev. D, 91, 123514
Chatterjee S. et al., 2017, Nature, 541, 58
Cordes J. M., Lazio T. J. W., 2002 preprint (arXiv:astroph/0207156)
Dai Z. G., Zhang B., Gou L. J., Mészáros P., Waxman E., 2002, ApJ, 580, L7
Dolag K., Gaensler B. M., Beck A. M., Beck M. C., 2015, MNRAS, 451, 4277
Dolag K., Grasso D., Springel V., Tkachev I., 2005, J. Cosmol. Astropart. Phys., 1, 9
Dolag K., Kachelrieß M., Ostapchenko S., Tomàs R., 2009, ApJ, 703, 1078
Donnert J., Dolag K., Lesch H., Müller E., 2009, MNRAS, 392, 1008
Federrath C., Schober J., Bovino S., Schleicher D. R. G., 2014, ApJ, 797, L19
Fialkov A., Loeb A., 2017, ApJ, 846, L27
Ghisellini G., Locatelli N., 2018, A&A, 613, A61
Hackstein S., Vazza F., Brüggen M., Sigl G., Dundovic A., 2016, MNRAS, 462, 3660
Hackstein S., Vazza F., Brüggen M., Sorce J. G., Gottlöber S., 2018, MNRAS, 475, 2519
Han J. L., 2017, ARA&A, 55, 111
Ioka K., 2003, ApJ, 598, L79
Kahniashvili T., Tevzadze A. G., Ratra B., 2011, ApJ, 726, 78
Keane E. F. et al., 2018, MNRAS, 473, 116
Kumar P., Lu W., Bhattacharya M., 2017, MNRAS, 468, 2726
Lorimer D. R., Bailes M., McLaughlin M. A., Narkevic D. J., Crawford F., 2007, Science, 318, 777
Lukić Z., Stark C. W., Nugent P., White M., Meiksin A. A., Almgren A., 2015, MNRAS, 446, 3697
Lyubarsky Y., 2014, MNRAS, 442, L9
Madau P., Dickinson M., 2014, ARA&A, 52, 415
McQuinn M., 2014, ApJ, 780, L33
Montanino D., Vazza F., Mirizzi A., Viel M., 2017, Phys. Rev. Lett., 119, 101101
Ng C., 2017, preprint (arXiv:1711.02104)
Oppermann N., Connor L. D., Pen U.-L., 2016, MNRAS, 461, 984
Petroff E. et al., 2015, MNRAS, 454, 457
Petroff E. et al., 2016, PASA, 33, e045
Petroff E. et al., 2017, MNRAS, 469, 4465
Planck Collaboration et al., 2016, A&A, 594, A13
Planck Collaboration XIX, A&A, 2016, 594, A19
Pshirkov M. S., Tinyakov P. G., Urban F. R., 2016, Phys. Rev. Lett., 116, 191302
Ryu D., Kang H., Cho J., Das S., 2008, Science, 320, 909
Sigl G., Miniati F., Ensslin T. A., 2003, Phys. Rev. D, 68, 043002
Subramanian K., 2016, Rep. Prog. Phys., 79, 076901
Thornton D. et al., 2013, Science, 341, 53
Trott C. M., Tingay S. J., Wayth R. B., 2013, ApJ, 776, L16
van Leeuwen J., 2014, in Wozniak P. R., Graham M. J., Mahabal A. A., Seaman R., eds, The Third Hot-wiring the Transient Universe Workshop, p. 79
Vazza F., Brunetti G., Brüggen M., Bonafede A., 2018, MNRAS, 474, 1672
Vazza F., Brüggen M., Gheller C., 2013, MNRAS, 428, 2366
Vazza F., Brüggen M., Gheller C., Hackstein S., Wittor D., Hinz P. M., 2017, Class. Quantum Gravity, 34, 234001
Vazza F., Brüggen M., Gheller C., Wang P., 2014, MNRAS, 445, 3706
Vazza F., Brüggen M., Wittor D., Gheller C., Eckert D., Stubbe M., 2016, MNRAS, 459, 70
Vazza F., Ferrari C., Brüggen M., Bonafede A., Gheller C., Wang P., 2015, A&A, 580, A119
Vernstrom T., Gaensler B. M., Brown S., Lenc E., Norris R. P., 2017, MNRAS, 467, 4914
Walker C. R. H., Ma Y.-Z., Breton R. P., 2018, preprint (arXiv:1804.01548)
Walters A., Weltman A., Gaensler B. M., Ma Y.-Z., Witzemann A., 2018, ApJ, 856, 65
Widrow L. M., Ryu D., Schleicher D. R. G., Subramanian K., Tsagas C. G., Treumann R. A., 2012, Space Sci. Rev., 166, 37
Xu H., Li H., Collins D. C., Li S., Norman M. L., 2009, ApJ, 698, L14
Xu J., Han J. L., 2015, Res. Astron. Astrophys., 15, 1629
Zandanel F., Fornasa M., Prada F., Reiprich T. H., Pacaud F., Klypin A., 2018, MNRAS, preprint (arXiv:1804.07063)

This paper has been typeset from a TEX/LATEX file prepared by the author.